The Vitreous Glycoprotein Opticin Inhibits Preretinal Neovascularization

Magali M. Le Goff,[1] *Hongbin Lu,*[1] *Marta Ugarte,*[1,2] *Stephen Henry,*[3] *Masamine Takanosu,*[4] *Richard Mayne,*[4] *and Paul N. Bishop*[1,2]

Purpose. Opticin is an extracellular matrix glycoprotein that the authors discovered in the vitreous humor of the eye. It is synthesized by the nonpigmented ciliary epithelium and secreted into the vitreous cavity and, unusually for an extracellular matrix molecule, high-level synthesis is maintained into adult life. Here the authors investigated the hypothesis that opticin influences vascular development in the posterior segment of the eye and pathologic angiogenesis into the normally avascular, mature (secondary) vitreous.

Methods. Opticin was localized in murine eyes by immunohistochemistry. An opticin knockout mouse was established and vascular development was compared between knockout and wild-type mice. Wild-type and opticin null mice were compared in the oxygen-induced retinopathy model, a model of pathologic angiogenesis, and this model was also used to assess the effects of intravitreal injection of recombinant opticin into eyes of wild-type mice.

Results. Opticin colocalizes with the collagen type II–rich fibrillar network of the vitreous, the inner limiting lamina, the lens capsule, the trabecular meshwork, and the iris. Analyses of the hyaloid and retinal vasculature showed that opticin has no effect on hyaloid vascular regression or developmental retinal vascularization. However, using the oxygen-induced retinopathy model, the authors demonstrated that opticin knockout mice produce significantly more preretinal neovascularization than wild-type mice, and the intravitreal delivery of excess opticin inhibited the formation of neovessels in wild-type mice.

Conclusions. A lack of opticin does not influence vascular development, but opticin is antiangiogenic and inhibits preretinal neovascularization. (*Invest Ophthalmol Vis Sci.* 2012;53:228–234) DOI:10.1167/iovs.11-8514

Opticin is a glycoprotein that we discovered associated with vitreous humor collagen fibrils.[1] Subsequently, it has been identified in other tissues including the brain and cartilage.[2,3] Opticin is a member of the extracellular matrix (ECM) small leucine-rich repeat protein/proteoglycan family[4,5] and is uniquely glycosylated via a cluster of sialylated O-linked oligosaccharides.[1] In solution it is a 90-kDa homodimer that dimerizes through its leucine-rich repeats.[6] Opticin is secreted into the vitreous by the posterior nonpigmented ciliary epithelium,[7] and during development expression is switched on as the nonpigmented ciliary epithelium differentiates (i.e., at about embryonic day 15.5 in the mouse eye).[8] Unusually for an ECM molecule,[9] high-level expression is maintained in the adult eye.[10] Little is known about the functions of opticin but it has been reported to interact with heparan and chondroitin sulfate glycosaminoglycans and retinal growth hormone.[11,12]

During eye development, the primary vitreous contains the hyaloid vessels, the vasa hyaloidea propria (VHP), and this supplies a network of vessels on the developing lens called the tunica vasculosa lentis (TVL).[13] The primary vitreous, VHP, and TVL undergo programed regression shortly after birth in mice (and before birth in humans) where they are replaced by the transparent, virtually acellular, secondary (mature) vitreous. The mature vitreous humor is a gel-like structure that normally demonstrates antiangiogenic properties.[14] However, in conditions including proliferative diabetic retinopathy (PDR) and retinopathy of prematurity (ROP), high levels of proangiogenic growth factors, especially vascular endothelial growth factor, switch the vitreous into a proangiogenic state and preretinal neovascularization occurs. Preretinal neovascularization is an angiogenic process whereby new blood vessels grow from the preexisting retinal vasculature into the vitreous.[15,16]

Given the high-level expression of opticin in the eye throughout life we speculated that it has functions in the vitreous other than simply being a structural ECM component. In particular, we hypothesized that opticin might influence developmental changes in blood vessels in the vitreous cavity and retina, and pathologic processes in which blood vessels grow into the vitreous. We explored these hypotheses using opticin knockout mice, and to investigate pathologic angiogenesis, the oxygen-induced retinopathy (OIR) model.[17] We demonstrated that although opticin does not influence vascular development, it does inhibit pathologic angiogenesis.

Methods

Materials

Recombinant bovine opticin was expressed using a mammalian system and purified as previously described.[6,11] A murine opticin peptide (TLSIEDYNEVIDLSNYEELADYGDQIPEAK) was used to generate rabbit polyclonal antiserum and the antibody was then affinity-purified against the peptide. A sheep anti-mouse collagen II antibody and goat anti-mouse endostatin and pigment epithelium–derived factor (PEDF) antibodies were purchased (R&D Systems, Abingdon, UK). The horseradish peroxidase (HRP)-conjugated and biotinylated secondary antibodies were all obtained for use (Sigma, Dorset, UK). Biotinylated

From [1]The School of Biomedicine, University of Manchester and the [2]Manchester Royal Eye Hospital and Centre for Advanced Discovery and Experimental Therapeutics, Central Manchester University Hospitals NHS Foundation Trust, Manchester Academic Health Sciences Centre, Manchester, United Kingdom; the [3]University of Texas MD Anderson Cancer Center, Houston, Texas; and the [4]Department of Cell Biology, University of Alabama, Birmingham, Alabama.

Supported in part by Wellcome Trust Grant 057940 (PNB), Manchester National Institute for Health Research Biomedical Research Centre, Manchester Royal Eye Hospital, the EyeSight Foundation of Alabama, and National Institutes of Health Grant R37 AR30481.

Submitted for publication September 1, 2011; revised November 19, 2011; accepted November 30, 2011.

Disclosure: **M.M. Le Goff**, None; **H. Lu**, None; **M. Ugarte**, None; **S. Henry**, None; **M. Takanosu**, None; **R. Mayne**, None; **P.N. Bishop**, P

Corresponding author: Paul N. Bishop, A.V. Hill Building, University of Manchester, Oxford Road, Manchester M13 9PT, UK; paul.bishop@manchester.ac.uk.

isolectin B4 and dye-conjugated streptavidin were obtained (Alexa Fluor 488 nm; Molecular Probes/Invitrogen, Paisley, UK).

Generation of Opticin Knockout Mice

A targeting vector was designed to replace a 5-kb region of the mouse opticin gene that spanned from exon 1 to exon 4, including the endogenous start site with a PGK-neomycin selection cassette flanked by loxP sites (a gift from Dr. R. Behringer, University of Texas). The homologous arms of the targeting vector were generated from PCR reactions using BAC DNA template (BAC clone previously identified from screening a BAC 129S7 library and known to contain the opticin gene). The linearized targeting vector contained an MC-1 TK cassette for negative selection, a 1.96-kb 5′ homologous arm, a floxed neomycin cassette, and a 3.75-kb 3′ homologous arm. The targeting vector was electroporated into AB2.2 embryonic stem (ES) cells (a gift from Dr. A. Bradley, Wellcome Trust Sanger Institute, Hinxton, UK) and cultured under positive and negative selection according to standard procedures. ES clones were screened for successful homologous recombination by Southern blotting with radiola-

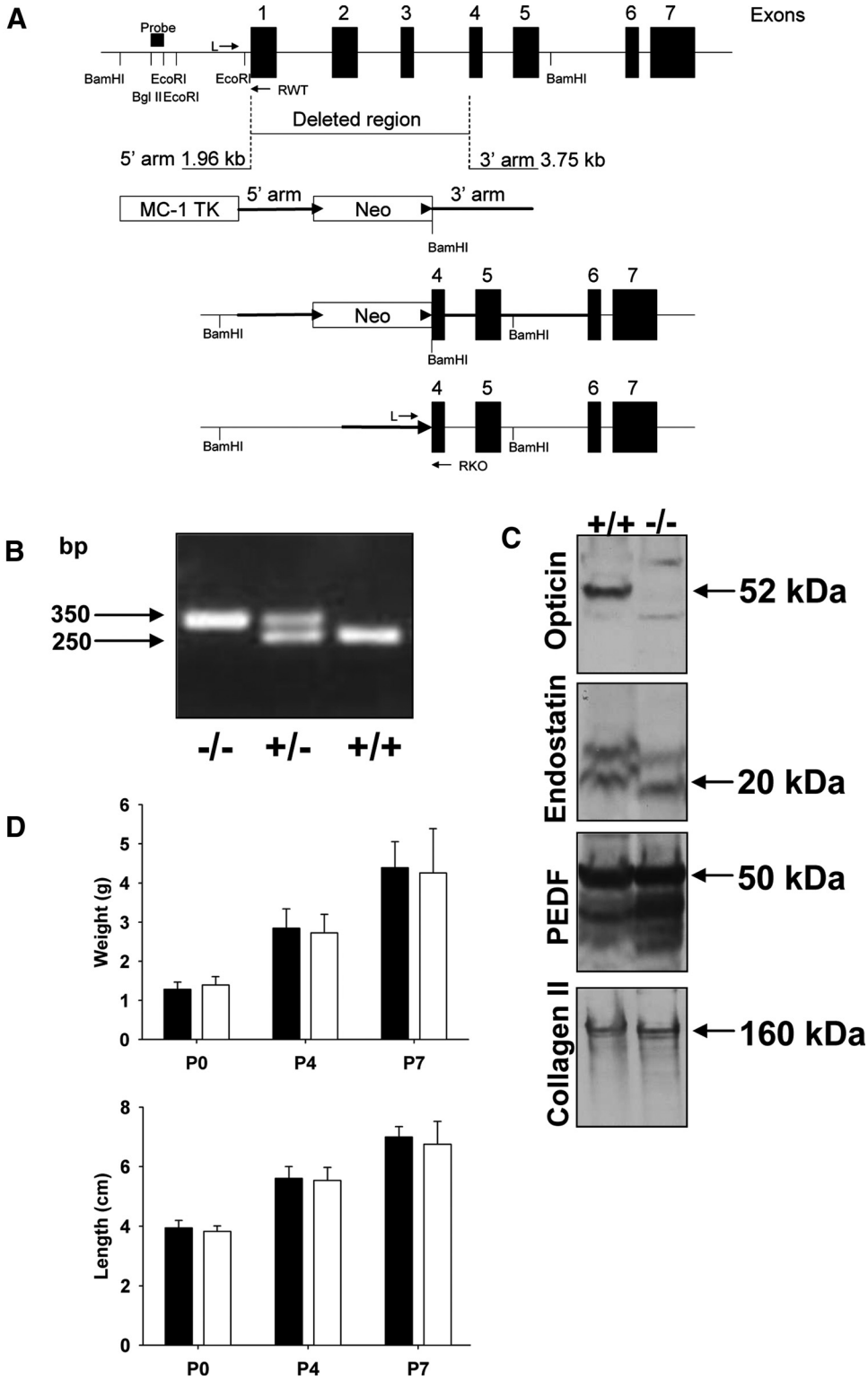

FIGURE 1. Generation of *Optc*−/− mice. (**A**) Genomic structure of mouse opticin indicating region deleted in *Optc*−/− mice and the arms obtained by PCR of an opticin containing BAC clone. *Bam*HI, *Eco*RI, and *Bgl*II restriction sites and the position for Southern-blotting analysis probe are indicated. The second diagram shows the targeting vector including MC-1 TK cassette for negative selection, 5′ and 3′ arms for recombination, and neomycin (Neo) cassette flanked with two floxed sites (*arrowheads*). The third diagram shows the inserted neomycin cassette within the targeted gene and the *bottom diagram* shows the deleted gene after Cre recombination to remove the neomycin cassette. Position of genotyping primers (L, RWT, and RKO) are shown on the *top* and *bottom panels*. (**B**) Electrophoresis separation of genotyping PCR products showed knockout (−/−), heterozygous (+), and wild-type (+/+) genotypes with their respective sizes in bp. (**C**) Extracts of *Optc*+/+ and *Optc*−/− mice whole eyes were separated by SDS-PAGE and analyzed by Western blotting with antibodies to opticin, endostatin, PEDF, and collagen type II; the arrows indicate the positions of these components with the corresponding molecular weight. Equal sample loading was checked by comparing the band intensities after collagen type II detection. (**D**) The growth of *Optc*+/+ (*black bars*) and *Optc*−/− (*white bars*) mice was compared by measuring weight and length at different postnatal stages ($n = 26$ [P0], $n = 65$ [P4], and $n = 68$ [P7] for *Optc*+/+ and $n = 11$ [P0], $n = 78$ [P4], and $n = 34$ [P7] for *Optc*−/−). No significant difference in either of the parameters could be seen between the animals ($P = 0.178$ at P0, $P = 0.092$ at P4, $P = 0.866$ at P7 for weight, and $P = 0.182$ at P0, $P = 0.327$ at P4, $P = 0.375$ at P7 for length).

beled 5′ probe (a 200-bp *Bgl*II/*Eco*RI fragment) that detects a 9.5-kb *Bam*HI fragment at the wild-type allele and a 5-kb *Bam*HI fragment at the mutant allele. Three targeted clones were identified and injected into blastocysts according to standard procedures, but only one resulted in germ line transmission as subsequently confirmed by PCR reactions. The F2 hybrid progeny (129S7/C57BL/6) containing the mutant opticin allele was backcrossed for 10 generations onto a C57BL/6 background to generate congenic opticin-null mice. The floxed neomycin cassette was removed by breeding with a cre-deleter mouse (a gift from Dr. A. Nagy, Toronto, Canada) maintained on a partial C57BL/6 background. Subsequent breeding was performed to select mice that were heterozygous and missing both neo and cre. Genomic DNA was extracted from mouse ear punches using a tissue extraction kit (Extract-N-Amp tissue PCR kit; Sigma). Left (L) and right (RKO) primers flanking the deleted DNA sequence and a second right (RWT) primer within the deleted fragment were designed and used for PCR genotyping. The sequence of the primer L was 5′-TCC AAG AAA CCT CAG CTT GG-3′, RKO was 5′-ATG TTC TCC AGG TCT GCA TC-3′, and RWT was 5′-TTG GCC AGG GAT GCA TGT GT-3′. After an initial denaturation at 95°C for 10 minutes, the PCR conditions were as follows: denaturation at 94°C for 40 seconds, annealing at 56°C for 30 seconds, and extension at 72°C for 1 minute for 35 cycles, followed by a final extension at 72°C for 10 minutes. The PCR products were then analyzed by electrophoresis on a 1.5% agarose gel. PCR amplification using the L/RKO primers combination gave a product of 350 base pairs (bp) indicating a null genotype and the L/RWT gave a product of 250 bp with the intact allele. The rate of mating, lethality, and number of offspring per litter were comparable between wild-type (*Optc*+/+), heterozygote, and knockout (*Optc*−/−) animals. Growth including weight and length of both wild-type and knockout animals was also monitored. All procedures involving animals were conducted in conformity to the ARVO statement for the use of animals in Ophthalmic and Vision Research and analyses of the mice were carried out in accordance with Institutional and United Kingdom Home Office guidelines under Project License 40/2819.

Western Blot Analysis

Eyes from *Optc*+/+ and *Optc*−/− mice were extracted with 8 M urea and the extracts subjected to 4–12% Bis-Tris gradient SDS-PAGE. Western blotting analysis was performed as previously described using a chemiluminescence detection system (PerkinElmer, Cambridge, UK).[18] Equal sample loading was checked by probing membranes with anti-mouse collagen type II antibody.

Histology Including Immunohistochemistry

Eyes from *Optc*+/+ and *Optc*−/− (used as negative control) mice at postnatal day 7 (P7) and *Optc*+/+ adult albino mice were fixed in 4% paraformaldehyde (PFA) before being embedded in paraffin. Sections (5 μm) were incubated with affinity-purified anti-mouse opticin antibody followed by a biotinylated anti-rabbit secondary antibody or with sheep anti-collagen II antibody followed by a biotinylated anti-sheep secondary antibody. The detection was performed using a commercial kit and substrate (Vectastain Universal elite ABC kit and Vector VIP substrate; Vector Laboratories, Peterborough, UK). Images were collected on an upright microscope (Axioskop; Carl Zeiss AG, Oberkochen, Germany) and captured using a microscope camera through an appropriate software program (AxioCam camera and AxioVision software; Carl Zeiss Microscopy). Images were then processed using ImageJ bioimaging software (developed by Wayne Rasband, National Institutes of Health, Bethesda, MD; available at http://rsb.info.nih.gov/ij/index.html).

To quantify the number of vessels forming the hyaloid vasculature and the extent of preretinal neovascularization after exposure to the OIR model, eyes were embedded in paraffin, after 4% PFA fixation, and 5-μm sections were cut and stained with hematoxylin and eosin (H&E). Analyses were carried out in a masked fashion. To analyze developmental vascular regression vessels were counted manually on every fifth section through the entire globe for the TVL and for 100 μm from the optic disc for the VHP. Quantification of preretinal neovascularization in the OIR model was undertaken using two different histology-based techniques. In one method the number of endothelial cells (ECs) above the inner limiting membrane (ILM) was counted on six sections that passed through the optic nerve and were 30 μm apart; ECs associated with hyaloid vasculature were easily distinguishable and these were not counted. A second method was to count the ECs on the vitreal side of the ILM on eight sections, 30 μm apart, starting 100 μm from the edge of the optic nerve head; this gave virtually identical results so the data are not shown.

Murine Oxygen-Induced Retinopathy Model

This is a well-established model for studying preretinal neovascularization.[17] Litters of P7 mice with their nursing dam (*Optc*−/− or *Optc*+/+) were placed in a 75% oxygen atmosphere for 5 days. At P12, the pups were returned to normal atmospheric conditions. In some experiments *Optc*+/+ mice were subjected to high oxygen between P7 and P12 as described earlier and then at day 14, one eye was injected intravitreally with recombinant opticin (2.5 μg in 1 μL of PBS), whereas the contralateral eye was injected with 1 μL of PBS only. The animals were euthanized at P12 or P17 and the eyes were enucleated for either fluorescent or H&E staining.

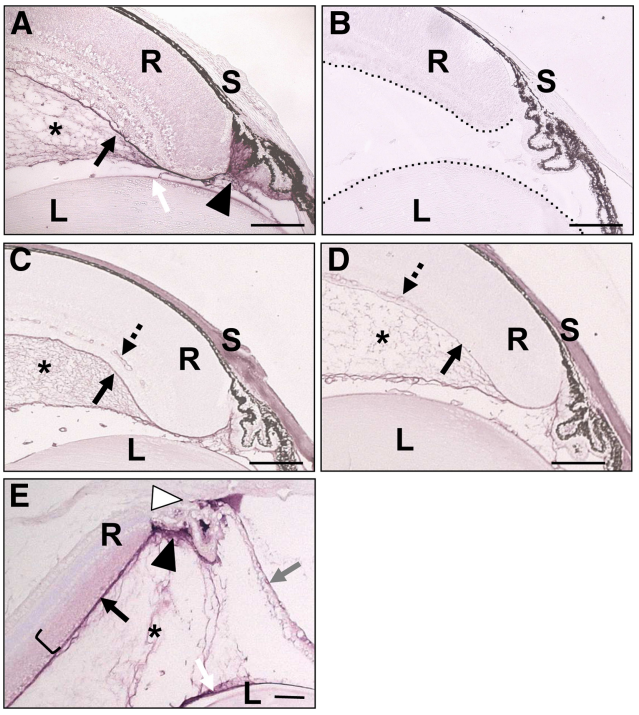

Figure 2. Localization of opticin in the mouse eye. (**A**) Immunolocalization with opticin antibody in P7 *Optc*+/+ eyes showed colocalization with vitreous collagen (*asterisk*), with intense staining adjacent to the nonpigmented ciliary epithelium (*filled triangle*). Labeling was also associated with the ILM (*black arrow*), the lens capsule (*white arrow*), and weak, diffuse staining was present in the retina. (**B**) No staining for opticin was observed in P7 *Optc*−/− eyes; the boundaries of the retina and lens are highlighted (*dashed line*). Immunolocalization using an anti-collagen type II antibody in P7 *Optc*+/+ (**C**) and *Optc*−/− (**D**) eyes highlighted the collagen network of the vitreous (*asterisk*). The antibody to collagen type II, probably due to cross-reactivity with other collagens, also stained the ILM (*black arrow*), retinal blood vessel walls (*dashed arrow*), and the sclera. (**E**) Immunolocalization of opticin in adult *Optc*+/+ albino eyes showed labeling of the vitreous (*asterisk*), especially adjacent to the posterior nonpigmented ciliary epithelium (*filled triangle*), the ILM (*black arrow*), the lens capsule (*white arrow*), the trabecular meshwork/anterior angle (*open triangle*), the inner layers of the neurosensory retina (*bracket*), and the iris (*gray arrow*). L, lens; R, retina; S, sclera. Scale bar: 100 μm.

Fluorescent Staining of the Retinal Vasculature

Eyes from *Optc*+/+ and *Optc*−/− mice at P4 and P7, and at P12 and P17 when subjected to the OIR model were fixed in 4% PFA after careful removal of the cornea and lens. After extensive washing with PBS containing 1% Triton X-100/1 mM $CaCl_2$/1 mM $MgCl_2$/0.1 mM $MnCl_2$, the eye cups were incubated with wash buffer containing 1% BSA followed by biotinylated isolectin B4 and finally with dye-conjugated streptavidin (Alexa Fluor 488). Retinas were then carefully removed from eye cups and flat-mounted with commercial mounting solution (Vectashield Set Mounting Solution; Vector Laboratories, Peterborough, UK). Images were acquired using a fluorescence microscope (Leica DFC420; Leica Microsystems) in conjunction with appropriate software (Leica Application Suite, version 3.3.0). Quantification of vascular coverage on the retina in eyes from *Optc*+/+ and *Optc*−/− mice at P4 and P7 was performed by evaluating the percentage of vascularized area versus the total area on the retinal surface using ImageJ software. In eyes from *Optc*+/+ and *Optc*−/− mice at P12 and P17 after exposure to the OIR conditions, the extent of the vaso-obliteration (VO) and preretinal neovascularization (NV) were quantified using specially designed software (SWIFT_NV software designed by Stahl and colleagues[19]).

Statistical Analysis

Results in figures were expressed as mean ± SD. The statistical analyses were undertaken using Student's *t*-tests, with $P < 0.05$ being considered significant.

Results

Generation of the *Optc*−/− Mouse

The mouse opticin gene contains 7 exons.[8] The *Optc*−/− mouse was generated by deleting exons 1 to 3 and part of exon 4 (Fig. 1A). This 5-kb deletion was confirmed by Southern blotting (data not shown) and genotyping was checked by PCR, with products of 250 and 350 bp indicating *Optc*+/+ and *Optc*−/− genotypes, respectively (Fig. 1B). Western blot analysis of proteins extracted from whole eyes of *Optc*+/+ and *Optc*−/− mice revealed a band at the expected size for opticin (~50 kDa by SDS-PAGE analysis) in *Optc*+/+ mice only (Fig. 1C). Western blot analyses for two other vitreous components, which have been shown to possess antiangiogenic properties (i.e., endostatin and PEDF), suggested that the absence of opticin did not alter their expression levels in the eye (Fig. 1C). No significant differences were observed in growth (i.e., weight and length) between *Optc*+/+ and *Optc*−/− mice at P0, P4, P7, or in older animals (Fig. 1D and data not shown).

Localization of Opticin in the Mouse Eye

Immunohistochemistry demonstrated opticin colocalization with the collagen type II–rich network in the vitreous (Figs. 2A, 2C, 2E). The opticin labeling was particularly intense adjacent to the nonpigmented ciliary epithelium, this being compatible with opticin being secreted by these cells into the vitreous

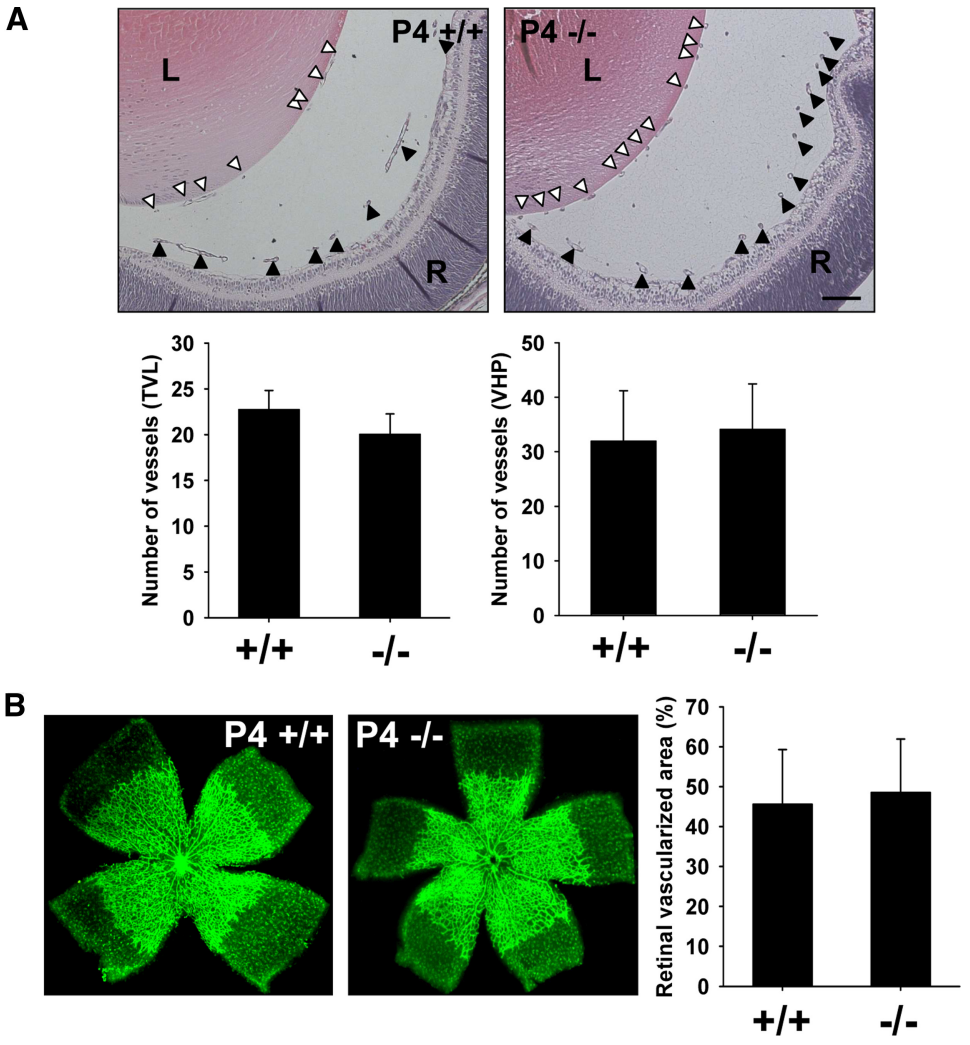

Figure 3. Effects of lack of opticin on hyaloid and retinal vasculature. (**A**) Quantification of the number of blood vessels in the TVL (*open triangle*) and VHP (*filled triangle*) on P4 *Optc*+/+ ($n = 10$) and *Optc*−/− ($n = 10$). H&E-stained eye sections showed no significant difference in the TVL ($P = 0.096$) or VHP ($P = 0.601$; scale bar: 100 μm). (**B**) Measurement of the proportion of the total retina that was vascularized on retinal flat-mounts after fluorescent isolectin staining in P4 *Optc*+/+ and *Optc*−/− showed no significant difference in retinal vascularization between *Optc*+/+ ($n = 81$) and *Optc*−/− ($n = 47$) mice ($P = 0.237$).

cavity (Figs. 2A, 2E). The anti-opticin antibody also strongly labeled the ILM and the lens capsule, indicating high concentrations of opticin localized to basement membranes. Weak, diffuse labeling was also observed in the neurosensory retina, particularly in the inner layers (Figs. 2A, 2E). In addition, opticin labeling was seen in the trabecular meshwork, particularly in albino adult eyes, and on the anterior surface of the iris (Fig. 2E). No staining for opticin was observed in *Optc*−/− mouse eye sections, indicating antibody specificity (Fig. 2B), but the vitreous collagen network was present (Fig. 2D).

Effects of Opticin on Vascular Development

The VHP and TVL of *Optc*+/+ and *Optc*−/− mice were compared and no significant differences in vessel number were observed at P0 (i.e., in the formation of hyaloid vasculature; data not shown) or during its regression at P4 (Fig. 3A). As the VHP and TVL regress the retinal vasculature develops by radiating outward from the optic disc reaching the retinal periphery by P7. Analyses of the area of vascularized retina on flat-mounts at P4 (Fig. 3B) and P7 (data not shown) showed no significant difference between *Optc*−/− and *Optc*+/+ mice. Therefore the lack of opticin does not influence hyaloid formation and regression or retinal vascularization.

Effects of Opticin on Pathologic Angiogenesis

We compared *Optc*+/+ and *Optc*−/− mice using the OIR model first described by Smith et al.[17] P7 mice are exposed to a high oxygen environment until P12 and after a 5-day period they are returned to normoxia. During the hyperoxic period, capillaries in the central area of the retina regress, leaving a central region of VO.[20] The return to normoxic conditions leads to a hypoxic response with a release of angiogenic growth factors, resulting in NV and revascularization of the avascular central retina. Analysis of VO at OIR P12 showed a decrease in the avascular area in *Optc*−/− mice compared with *Optc*+/+ animals (Fig. 4A); however, at this time point there was no significant difference in the number of vessels in the VHP or TVL (Fig. 4B). Analysis of the central avascular zone at OIR P17 showed that the reduced area of VO in the *Optc*−/− compared with *Optc*+/+ mice was also present at this time point (Figs. 5A, 5B). The NV peaks at OIR P17 in this model,[17] so we analyzed this response using two independent methods (see the Methods section). Both methods of quantification revealed that the *Optc*−/− mice develop significantly more NV compared with their wild-type counterparts (Figs. 5A, 5C, 5D). Because the weight of the animals at OIR 17 may correlate with the severity of ROP,[20,21] the weights of the *Optc*+/+ and *Optc*−/− mice were compared, although no significant difference was found (Fig. 5E).

Further experiments were undertaken in which *Optc*+/+ mice were injected intravitreally with opticin at OIR P14 and the contralateral eye was injected with carrier buffer (PBS) alone. Analysis of VO showed no significant difference between PBS and opticin injection at OIR P17 (data not shown), revealing that opticin has no effect on the revascularization of the central avascular retinal area. The extent of neovascularization was analyzed using two independent methods and both quantifications showed that at OIR P17 there was significantly less preretinal neovascularization in the opticin-injected eyes compared with control eyes (Fig. 5F and data not shown).

Discussion

In this study we demonstrated that opticin colocalizes with vitreous collagen fibrils. Opticin also localized to the ILM and

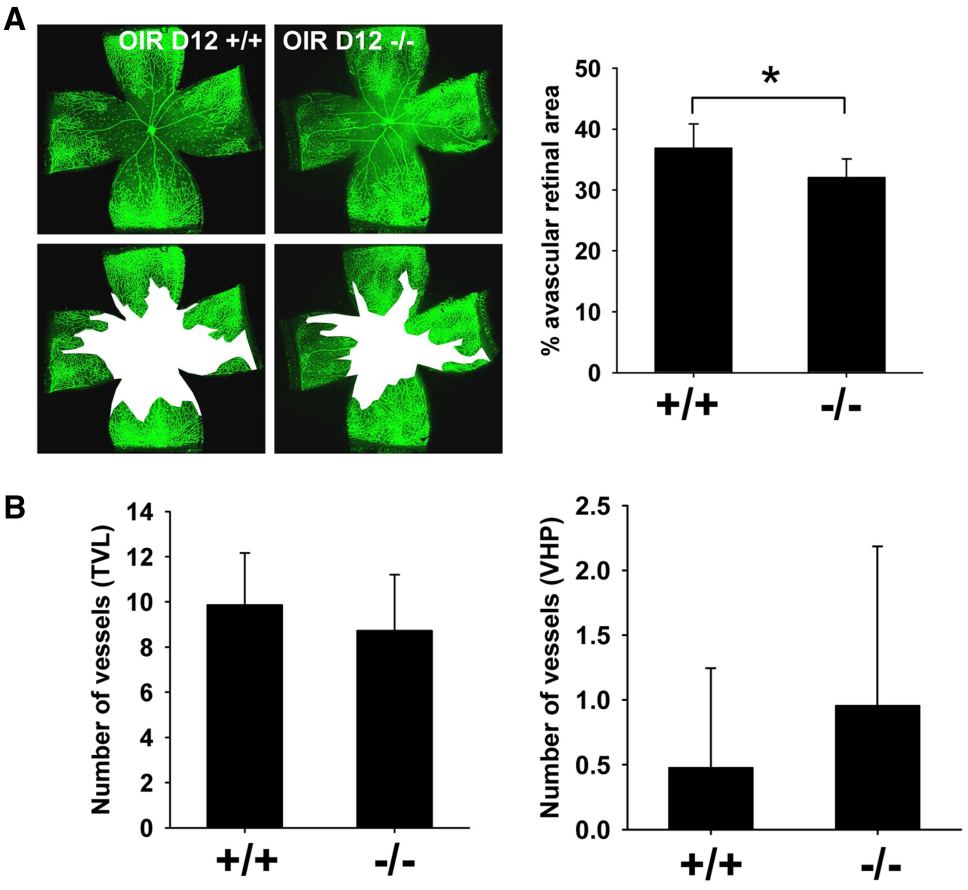

Figure 4. *Optc*−/− mice display a decrease in vaso-obliteration in the oxygen-induced retinopathy model at P12. (**A**) *Optc*+/+ and *Optc*−/− animals were subjected to the OIR model and euthanized at P12. The central avascular area was outlined in *white* after fluorescent isolectin staining at OIR P12 and quantification was performed as a percentage of the total retinal area. This revealed a 13% decrease in vaso-obliteration in *Optc*−/− ($n = 10$) compared with *Optc*+/+ ($n = 7$) mice and this was statistically significant ($^*P = 0.012$). (**B**) Quantification of the number of vessels in TVL and VHP after H&E staining of eye sections at this stage showed no significant difference between *Optc*+/+ ($n = 7$) and *Optc*−/− ($n = 10$) ($P = 0.348$ for TVL and $P = 0.390$ for VHP).

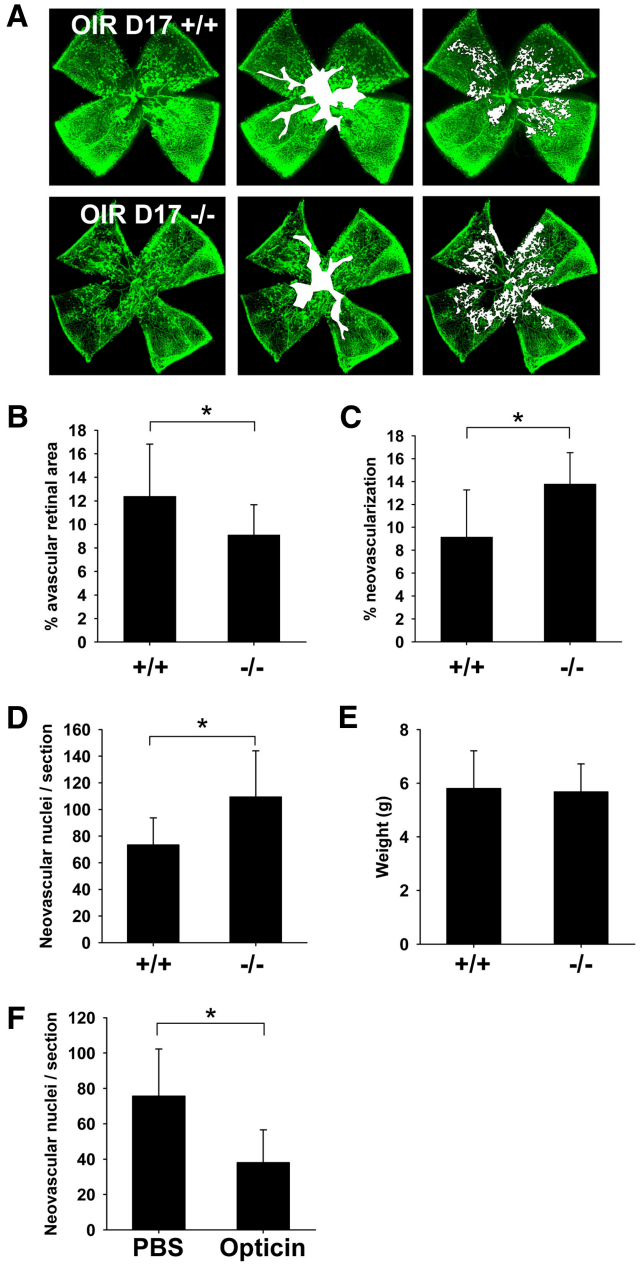

FIGURE 5. *Optc*−/− mice display an increase in preretinal neovascularization in the oxygen-induced retinopathy model at P17. (**A**) *Optc*+/+ and *Optc*−/− mice were subjected to the OIR model and then analyzed at P17. Quantification of vaso-obliteration (outlined in *white* in *middle panel*) and preretinal neovascularization (highlighted with *white dots* in *right panel*) was performed on retinal flat-mounts after fluorescent isolectin staining (using SWIFT_NV software) and reported as a percentage of total retinal area. (**B**) There was a significantly less (26%) vaso-obliteration in the *Optc*−/− mice (n = 37/from 3 litters) compared with the *Optc*+/+ counterparts (n = 20/from 3 litters) (*P = 0.006). (**C**) The *Optc*−/− mice (n = 37/from 3 litters) demonstrated 51% more preretinal neovascularization than the *Optc*+/+ mice (n = 20/from 3 litters) (*$P < 0.001$). (**D**) The neovascular response at OIR P17 was also quantified by counting ECs in preretinal vascular tufts on H&E-stained eye sections and revealed that *Optc*−/− mice (n = 8/from 2 litters) developed 46% more preretinal ECs than *Optc*+/+ mice (n = 8/from 3 litters) (*$P < 0.001$). (**E**) The weight of *Optc*+/+ (n = 15) and *Optc*−/− (n = 26) mice was measured at P17 after being subjected to the OIR model and there was no significant difference between both animals (P = 0.746). (**F**) In further experiments, one eye from *Optc*+/+ mice subjected to the OIR model was injected with recombinant opticin (n = 6/from 2 litters) at P14 and the contralateral eye with PBS (carrier buffer), then neovascular growth analyzed at P17 by counting ECs in preretinal vascular tufts on H&E-stained eye sections. Quantification of neovascularization revealed that eyes injected with opticin had 50% less preretinal ECs than PBS-injected control eyes (*$P < 0.001$). Similar opticin injection experiments (one eye receiving opticin and the contralateral eye buffer alone) were performed with *Optc*+/+ eyes (n = 6/from 1 litter), but quantification of vaso-obliteration and preretinal neovascularization was performed on retinal flat-mounts after fluorescent isolectin staining (SWIFT_NV software). No significant difference could be observed between both groups in the hyperoxic-driven vaso-obliterative response (P = 0.960), but the opticin injected *Optc*+/+ eyes developed significantly less preretinal neovascularization compared with PBS control ($P < 0.001$) (data not shown).

lens capsule, as we have previously observed in the human eye.[18] In addition, low levels of opticin were detected in the neurosensory retina, particularly in its inner layers, confirming data previously published in rat.[22] Because opticin is secreted by the nonpigmented ciliary epithelium,[8] this is likely to be due to opticin traversing the vitreous cavity and then passing through the ILM into the retina; there it may be immobilized by interactions with glycosaminoglycans such as heparan sulfate.[11] Opticin was also observed in the trabecular meshwork, confirming observations in the human eye,[23] and was more apparent in adult compared with young eyes, suggesting an age-related accumulation.

In the mouse, regression of the hyaloid vasculature begins at around the time of birth and is normally complete by about P20.[24] As the VHP and TVL regress the retinal vasculature develops by radiating outward from the optic disc, reaching the retinal periphery by P7. We hypothesized that opticin might affect this process as endostatin, another antiangiogenic molecule derived from ECM, promotes regression of the hyaloid vascular system.[25] However, the absence of opticin did not affect this process.

In normal conditions, the mature vitreous is avascular and this characteristic is crucial for clear vision. It has been recognized for decades that the vitreous is normally antiangiogenic,[14] and it is known to contain molecules that have antiangiogenic properties including PEDF, thrombospondin-1 (TSP-1), and endostatin.[26–28] Here we show that opticin is also an endogenous inhibitor of angiogenesis in the vitreous. Evidence for the antiangiogenic activity of PEDF, TSP-1, and endostatin in vitreous comes from experiments using the OIR model showing, as we have for opticin, that after intravitreal delivery of an excess of these molecules there is an approximately 50% inhibition of preretinal neovascularization.[29–31] However, the potential importance of opticin as an endogenous inhibitor of angiogenesis is highlighted by our experiments showing that *Optc*−/− mice exhibit increased preretinal neovascularization compared with *Optc*+/+ mice in the OIR model, whereas a lack of PEDF, TSP-1, or collagen XVIII/endostatin does not increase preretinal neovascularization in this model (Wiegand SJ, et al. *IOVS* 2004;45:ARVO E-Abstract 1884).[32,33] However, antiangiogenic factors including opticin, PEDF, TSP-1, and endostatin in the vitreous cavity may work in cooperation to prevent spontaneous vascularization and their effects become outweighed only when there is an extreme angiogenic drive in certain pathologic situations.

In *Optc*−/− mice subjected to the OIR model, we observed a smaller central avascular area at both OIR P12 and OIR P17 compared with *Optc*+/+ mice. It might be expected that a smaller avascular area would result in less angiogenic stimulus, but instead significantly more preretinal neovascularization was observed in the *Optc*−/− mice than that in *Optc*+/+ mice. The reason for the smaller avascular area in the *Optc*−/− mice is uncertain, but it is possible that the presence of opticin

in the retina enhances the hyperoxia-driven vasoobliterative process in the central retina. The injection of opticin in *Optc+/+* mice eyes at OIR P14 did not affect the size of the avascular area in the central retina at OIR P17, suggesting that the levels of opticin do not affect the rate of retinal revascularization. A potential explanation for opticin levels affecting preretinal neovascularization and vaso-obliteration in the OIR model is that it disrupts integrin-mediated EC interactions with collagens and laminin (Le Goff MM, et al. *IOVS* 2011;52:ARVO E-Abstract 4843). However, opticin does not disrupt integrin-mediated EC interactions with fibronectin, which have been shown to be important in both developmental retinal vascularization and revascularization in the OIR model.[34,35]

This study shows that opticin possesses an antiangiogenic function in the vitreous, and this antiangiogenic activity might explain why the nonpigmented ciliary epithelium continues to secrete opticin into the vitreous cavity throughout life. Furthermore, opticin or opticin-derived molecules, used alone or in combination with other reagents, may be useful as therapeutics for targeting pathologic angiogenesis.

Acknowledgments

The authors thank Glenn Ferris, Anne White, Kevin Pawlik, and staff at the Biological Services Facility (University of Manchester), especially Sarah Lawton, for their technical assistance, and Andreas Stahl and Lois Smith for kindly providing us with the SWIFT_NV software.

References

1. Reardon AJ, Le Goff MM, Briggs M, et al. Identification in vitreous and molecular cloning of opticin, a novel member of the family of leucine-rich repeat proteins of the extracellular matrix. *J Biol Chem.* 2000;275:2123–2129.
2. Frolova EI, Kokina VM, Beebe DC. The expression pattern of opticin during chicken embryogenesis. *Gene Expr Patterns.* 2004; 4:335–338.
3. Monfort J, Tardif G, Roughley P, et al. Identification of opticin, a member of the small leucine-rich repeat proteoglycan family, in human articular tissues: a novel target for MMP-13 in osteoarthritis. *Osteoarthritis Cartilage.* 2008;16:749–755.
4. Schaefer L, Iozzo RV. Biological functions of the small leucine-rich proteoglycans: from genetics to signal transduction. *J Biol Chem.* 2008;283:21305–21309.
5. McEwan PA, Scott PG, Bishop PN, Bella J. Structural correlations in the family of small leucine-rich repeat proteins and proteoglycans. *J Struct Biol.* 2006;155:294–305.
6. Le Goff MM, Hindson VJ, Jowitt TA, Scott PG, Bishop PN. Characterization of opticin and evidence of stable dimerization in solution. *J Biol Chem.* 2003;278:45280–45287.
7. Bishop PN, Takanosu M, Le Goff M, Mayne R. The role of the posterior ciliary body in the biosynthesis of vitreous humour. *Eye.* 2002;16:454–460.
8. Takanosu M, Boyd TC, Le Goff MM, et al. Structure, chromosomal location and tissue-specific expression of the mouse opticin gene. *Invest Ophthalmol Vis Sci.* 2001;42:2202–2210.
9. Halfter W, Dong S, Schurer B, Ring C, Cole GJ, Eller A. Embryonic synthesis of the inner limiting membrane and vitreous body. *Invest Ophthalmol Vis Sci.* 2005;46:2202–2209.
10. Wistow G, Bernstein SL, Ray S, et al. Expressed sequence tag analysis of adult human iris for the NEIBank Project: steroid-response factors and similarities with retinal pigment epithelium. *Mol Vis.* 2002;8:185–195.
11. Hindson VJ, Gallagher JT, Halfter W, Bishop PN. Opticin binds to heparan and chondroitin sulfate proteoglycans. *Invest Ophthalmol Vis Sci.* 2005;46:4417–4423.
12. Sanders EJ, Walter MA, Parker E, Aramburo C, Harvey S. Opticin binds retinal growth hormone in the embryonic vitreous. *Invest Ophthalmol Vis Sci.* 2003;44:5404–5409.
13. Saint-Geniez M, D'Amore PA. Development and pathology of the hyaloid, choroidal and retinal vasculature. *Int J Dev Biol.* 2004;48: 1045–1058.
14. Lutty GA, Thompson DC, Gallup JY, Mello RJ, Patz A, Fenselau A. Vitreous: an inhibitor of retinal extract-induced neovascularization. *Invest Ophthalmol Vis Sci.* 1983;24:52–56.
15. Heidary G, Vanderveen D, Smith LE. Retinopathy of prematurity: current concepts in molecular pathogenesis. *Semin Ophthalmol.* 2009;24:77–81.
16. Frank RN. Diabetic retinopathy. *N Engl J Med.* 2004;350:48–58.
17. Smith LEH, Wesolowski E, McLellan A, et al. Oxygen-induced retinopathy in the mice. *Invest Ophthalmol Vis Sci.* 1994;35:101–111.
18. Ramesh S, Bonshek RE, Bishop PN. Immunolocalisation of opticin in the human eye. *Br J Ophthalmol.* 2004;88:697–702.
19. Stahl A, Connor KM, Sapieha P, et al. Computer-aided quantification of retinal neovascularization. *Angiogenesis.* 2009;12:297–301.
20. Stahl A, Connor KM, Sapieha P, et al. The mouse retina as an angiogenesis model. *Invest Ophthalmol Vis Sci.* 2010;51:2813–2826.
21. Vanhaesebrouck S, Daniels H, Moons L, Vanhole C, Carmeliet P, De Zegher F. Oxygen-induced retinopathy in mice: amplification by neonatal IGF-1 deficit and attenuation by IGF-1 administration. *Pediatr Res.* 2009;65:307–310.
22. Hobby P, Wyatt MK, Gan W, et al. Cloning, modeling, and chromosomal localization for a small leucine-rich repeat proteoglycan (SLRP) family member expressed in human eye. *Mol Vis.* 2000;6: 72–78.
23. Friedman SJ, Faucher M, Hiscott P, et al. Protein localization in the human eye and genetic screen of opticin. *Hum Mol Genet.* 2002; 11:1333–1342.
24. Ito M, Yoshioka M. Regression of the hyaloid vessels and papillary membrane of the mouse. *Anat Embryol.* 1999;200:403–411.
25. Fukai N, Eklund L, Marneros AG, et al. Lack of collagen XVIII/endostatin results in eye abnormalities. *EMBO J.* 2002;21:1535–1544.
26. Dawson DW, Volpert OV, Gillis P, et al. Pigment epithelium-derived factor: a potent inhibition of angiogenesis. *Science.* 1999; 285:245–248.
27. Sheibani N, Sorenson CM, Cornelius LA, Frazier WA. Thrombospondin-1, a natural inhibitor of angiogenesis, is present in vitreous and aqueous humor and is modulated by hyperglycemia. *Biochem Biophys Res Commun.* 2000;267:257–261.
28. Määttä M, Heljasvaara R, Pihlajaniemi T, Uusitalo M. Collagen XVIII/endostatin shows a ubiquitous distribution in human ocular tissues and endostatin-containing fragments accumulate in ocular fluid samples. *Graefes Arch Clin Exp Ophthalmol.* 2007; 245:74–81.
29. Mori K, Duh E, Gehlbach P, et al. Pigment epithelium-derived factor inhibits retinal and choroidal neovascularisation. *J Cell Physiol.* 2001;188:253–263.
30. Zhang M, Yang Y, Yan M, Zhang J. Downregulation of vascular endothelial growth factor and integrin $\beta 3$ by endostatin in a mouse model of retinal neovascularisation. *Exp Eye Res.* 2006;82:74–80.
31. Wu Z, Wang S, Sorenson CM, Sheibani N. Attenuation of retinal vascular development and neovascularisation in transgenic mice over-expressing thrombospondin-1 in the lens. *Dev Dyn.* 2006; 235:1908–1920.
32. Wang S, Wu Z, Sorenson CM, Lawler J, Sheibani N. Thrombospondin-1-deficient mice exhibit increased vascular density during retinal vascular development and are less sensitive to hyperoxia-mediated vessel obliteration. *Dev Dyn.* 2003;228:630–642.
33. Hurskainen M, Eklund L, Hägg PO, et al. Abnormal maturation of the retinal vasculature in type XVIII collagen/endostatin deficient mice and changes in retinal glial cells due to lack of collagen types XV and XVIII. *FASEB J.* 2005;19:1564–1566.
34. Uemura A, Kusuhara S, Wiegand SJ, Yu RT, Nishikawa S. Tlx acts as a proangiogenic switch by regulating extracellular assembly of fibronectin matrices in retinal astrocytes. *J Clin Invest.* 2006;116: 369–377.
35. Maier AK, Kociok N, Zahn G, et al. Modulation of hypoxia-induced neovascularization by JSM6427, an integrin $\alpha 5\beta 1$ inhibiting molecule. *Curr Eye Res.* 2007;32:801–812.